ELSEVIER
Nuclear Instruments and Methods in Physics Research A 463 (2001) 653–662
NUCLEAR INSTRUMENTS & METHODS IN PHYSICS RESEARCH Section A
www.elsevier.nl/locate/nima

Neutron and fragment yields in proton-induced fission of ^{238}U at intermediate energies

V.A. Rubchenya[a,b,*], W.H. Trzaska[a], D.N. Vakhtin[b], J. Äystö[a], P. Dendooven[a], S. Hankonen[a], A. Jokinen[a], Z. Radivojevich[a], J.C. Wang[a], I.D. Alkhazov[b], A.V. Evsenin[b], S.V. Khlebnikov[b], A.V. Kuznetsov[b], V.G. Lyapin[a,b], O.I. Osetrov[b], G.P. Tiourin[b], A.A. Aleksandrov[c], Yu.E. Penionzhkevich[c]

[a] *Department of Physics, University of Jyväskylä, FIN-40351 Jyväskylä, Finland*
[b] *V.G. Khlopin Radium Institute, St.-Petersburg 194021, Russia*
[c] *Flerov Laboratory of Nuclear Reactions, 141980 Dubna, Russia*

Abstract

The primary fission fragment mass and kinetic energy distributions, and neutron multiplicities as function of fragment mass have been measured in the proton-induced fission of ^{238}U at energies $E_p = 20, 35, 50$ and 60 MeV using time-of-flight technique. Pre-scission and post-scission neutron multiplicities have been extracted from double differential distributions. The fragment mass dependence of the post-scission neutron multiplicities reveals the gross nuclear shell structure effect even at the higher proton energies we measured. The yields of neutron-rich fission products in the fission of ^{238}U by 25 MeV protons were measured using an ion guide-based isotope separator technique. The results indicate enhancement for superasymmetric mass division at intermediate excitation energy of the fissioning nucleus. The experimental results have been analysed in the framework of a time-dependent statistical model with inclusion of nuclear friction effects in the fission process.

PACS: 24-75.+i; 25-85.Ge; 29-30.Hs; 29-40.Cs; 29-40.Mc

Keywords: Proton-induced fission; Fission fragment yields; Fission neutron multiplicities; Statistical theory of fission; Time-of-flight technique

1. Introduction

A great deal of interest in the investigation of light-particles-induced fission of heavy nuclei at intermediate energy is connected with several important reasons. The first one is related to the problem of understanding the fission process with increasing excitation energy of the compound nucleus. Recently it was shown that the asymmetric character of the mass distribution in the fast-neutron-induced fission of ^{238}U is preserved at neutron energies up to about 100 Mev [1,2]. A large enhancement for superasymmetric mass division at $A < 80$ in the 25 MeV proton-induced fission of ^{238}U was observed [3] which supports the hypothesis about the existence of a superasymmetric fission mode. Determination of the most probable charge of fission products in the 24 MeV

*Corresponding author. Tel.: +358-14-260-2375; fax: +358-14-260-2351.
E-mail address: rubchen@phys.jyu.fi (V.A. Rubchenya).

0168-9002/01/$ - see front matter
PII: S0168-9002(01)00176-0

proton-induced fission of ^{238}U [4] demonstrates that charge polarization in the fission process is preserved up to a few tens of MeV of excitation energy of the compound nucleus.

The second reason is connected with the problem of obtaining exotic neutron-rich radioactive ion beams [5] when, in particular, a thick uranium target is irradiated by an intense secondary beam of fast neutrons from the break-up of high energy deuterons. Recently, new neutron-rich isotopes were observed in fission processes in ^{238}U-collisions on Pb and Be targets at relativistic energies [6,7].

The third reason is related to the technical application of nuclear reactions at intermediate energy for energy production and transmutation of nuclear waste in hybrid accelerator-driven systems [8–10]. Different reaction cross-sections and the specific radioactive decay properties of the reaction products are important for design and operation of such a subcritical reactor. Available data of the neutron and fragment yields are rather scarce for the proton-induced fission of ^{238}U in the energy range between 20 and 100 MeV [4,11–14].

The detailed theoretical calculation of the fission product formation cross-sections at intermediate energy consists of two parts: (i) modeling the reaction mechanism to calculate mass, charge, and excitation energy distributions of compound nuclei and (ii) modeling the fission process itself. For the case of light-particle-induced fission of heavy nuclei a theoretical model for calculation of independent fission product cross-sections was proposed and developed in our previous works [15–17]. Recently, a theoretical model for calculation of nuclide production yields in relativistic collisions was developed [18].

In this paper we present a study on the prompt neutron yields and fragment mass distributions in proton-induced fission of ^{238}U at $E_p = 20, 35, 50,$ and 60 MeV using the HENDES setup [19]. The neutron-rich fission product yields in ^{238}U(p, f) at $E_p = 25$ MeV were measured using the ion guide isotope separation technique IGISOL [20,21]. The experimental results were analyzed in the framework of a new version of the theoretical model which is a combination of a model for calculation of fission product yields proposed earlier in Refs. [15–17] and a time-dependent statistical model for

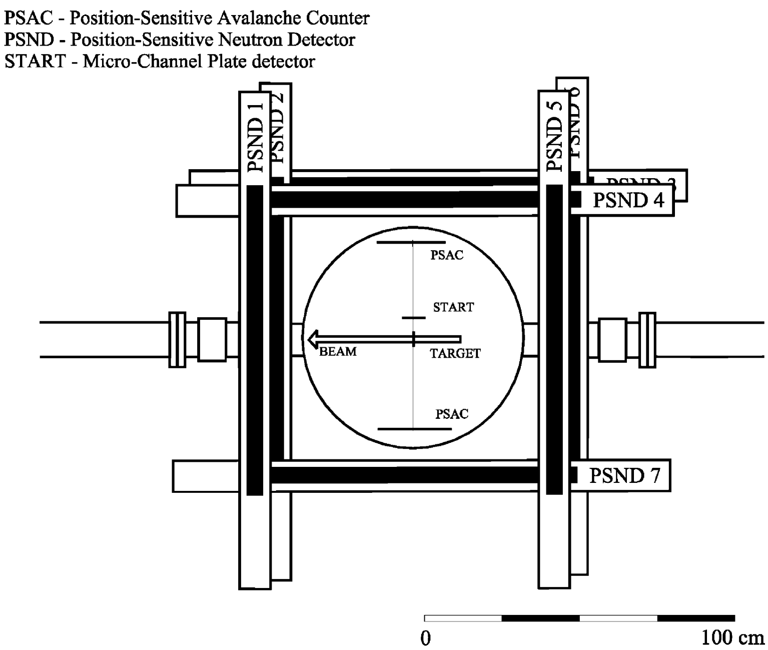

Fig. 1. Experimental lay-out of HENDES for the ^{238}U (p, fission) experiment (top view).

fission fission process with inclusion of dynamical effects [22].

2. Neutron and fragment measurements with HENDES

2.1. Experiment

The measurements were carried out using the High Efficiency Neutron DEtection System (HENDES) facility [19] at the Accelerator Laboratory, University of Jyväskylä. The scheme of the experimental setup is shown in Fig. 1. A $100\,\mu g/cm^2$ layer of ^{238}U evaporated on $60\,\mu g/cm^2$ thick Al_2O_3 backing was bombarded with 20, 35, 50 and 60 MeV proton beams. A typical beam spot dia-meter on the target was 5 mm, the average beam intensity was about 10 pnA. To measure double-differential neutron spectra (recording both energy and angle) in coincidence with fission fragments, seven position-sensitive neutron detectors (PSND), two large, position-sensitive avalanche counters (PSAC) and one micro-channel plate (MCP) start detector were used. The time-of-flight (TOF) method was used both for fission fragment and neutron detection. Sufficient statistics was needed to carry out reliable unfolding of the spectra into pre- and post-scission multiplicities.

Our PSAC detectors [23], having a time resolution of better than 400 ps, a position resolution below 1 mm and diameter of 245 mm, were tuned to be insensitive to α-particles. The MCP, with $100\,\mu g/cm^2$ thick gold plated mylar converter foil and intrinsic time resolution of 100 ps, was placed in front of one of the PSAC detectors. For both PSACs, the distance between cathode center and target was 235 mm. In-plane angles between the beam direction and the centers of the first and second PSAC were 90°. The angular acceptance of both detectors was 56° in-plane and $\pm 28^\circ$ out-of-plane. Both PSACs and MCP detector were placed inside a spherical stainless steel reaction chamber with a diameter of 80 cm and wall a thickness of 2 mm.

The neutron energy determination was also based on TOF technique. Each of the seven PSNDs [24,25] surrounding the chamber consisted of a 100 cm long quartz tube with a diameter of 6 cm filled with 2.3 l of NE-213 liquid scintillator, and enclosed by two photo-multipliers coupled directly to each end of the scintillator. The time resolution of PSND was measured with a collimated ^{60}Co γ-source to be 1.4 ns. Energy-dependent position resolution of the neutron detectors changed from 20 cm for 1 MeV neutrons to 10 cm for neutron energies of 4 MeV and above. This makes the set of seven PSNDs equivalent to 35 individual detectors. The intrinsic efficiency varied from 34% to 22% in the 1–10 MeV range, with the threshold set at 0.8 MeV. Neutron/γ separation was done with a standard pulse-shape technique. More details about the detector geometry are given in Table 1.

Before and after each measurement the whole detection system was tested and calibrated with a ^{252}Cf source. Threshold levels on PSND electronics were adjusted to 0.8 MeV of proton recoil energy. Measures were taken to minimize the background. No collimators were used in the vicinity of the target chamber. The beam dump, 3.5 m from the target, was shielded by 20 cm of paraffin (with boron) and 25 cm of lead. We have also estimated the influence of the reaction chamber and other surrounding materials on the registration of neutron spectra.

2.2. Data analysis and experimental results

The aim of the fission fragment data analysis was to determine the primary fragment masses m_1

Table 1
Distances and angles between target and center point of each detector

	PSND1	PSND2	PSND3	PSND4	PSND5	PSND6	PSND7	PSAC1	PSAC2	MCP
L (cm)	62	62	67	50	62	62	60	23.5	23.5	2
$\Theta_{in-pl}(^\circ)$	0	0	−90	−90	180	180	90	−90	90	−90
$\phi_{out-of-pl.}(^\circ)$	11	−11	−22	0	11	−11	0	0	0	0

and m_2 and the velocity vectors $\boldsymbol{v}_1$ and $\boldsymbol{v}_2$. Fission fragment velocity vectors in zero approximation, $\boldsymbol{v}_f^0$, were determined from time-of-flight and position information. The main source of systematic error at this stage was energy loss in the START detector converter foil and in the target.

The first approximation for fragment masses $m_{1,2}^0$ was calculated using momentum conservation perpendicular to the beam axis $m_1 v_1^{\perp} = m_2 v_2^{\perp}$ and assuming that the two fragment masses add up to the mass of the compound system prior to fission ($m_1 + m_2 = M_{\text{projectile}} + M_{\text{target}} - M^{\text{pre}}$), where M^{pre} is the mean total mass of the particles emitted from the compound nucleus before scission. Since neutrons dominate in pre-scission emission, M^{pre} was assumed to be equal to the neutron pre-scission multiplicity M_n^{pre}. The value of M_n^{pre} was first taken from theoretical calculations and, at a later stage, substituted with the experimental value. The influence of uncertainty in the M^{pre} determination turned out to be much smaller than the overall errors determined mostly by the time resolution of the PSACs.

From $\boldsymbol{v}_{1,2}^0$ and $m_{1,2}^0$, the fragment energies $E_{1,2}^0$ were determined using non-relativistic formulae. The known fragment mass and energy allowed one to calculate consequently the energy losses in the START detector and the target. From the corrected values of $E_{1,2}^1 = E_{1,2}^0 + \Delta E^{\text{START}} + \Delta E^{\text{target}}$ and the old values of fragment masses $m_{1,2}^0$, new values of the fragment velocities "in the target" were calculated; the above procedure was repeated until it converged. Usually two iterations were sufficient.

Using the extracted values of $\boldsymbol{v}_{1,2}^0$ and $m_{1,2}$, the experimental laboratory velocity of the compound nuclear system $\boldsymbol{V}_{\text{CN}}$, the fragment velocities in the center of mass, and the total kinetic energy (TKE) distribution of the fission fragments were calculated. Experimentally obtained values of the averaged kinetic energies and the full-widths at half-maximum (FWHM) are summarized in Table 2. The obtained mass distributions of the fission fragments prior to post-scission neutron emission for four proton energies $E_p = 20, 35, 50$ and 60 MeV (*symbols*) together with the model calculations (*lines*) are shown in Fig. 2.

Table 2
The measured total fission fragment kinetic energies and their FWHM

E_{lab} (MeV)	TKE (MeV)	FWHM (MeV)
20	168.2	27.3
35	171.4	27.5
50	171.6	28.2
60	174.0	29.0

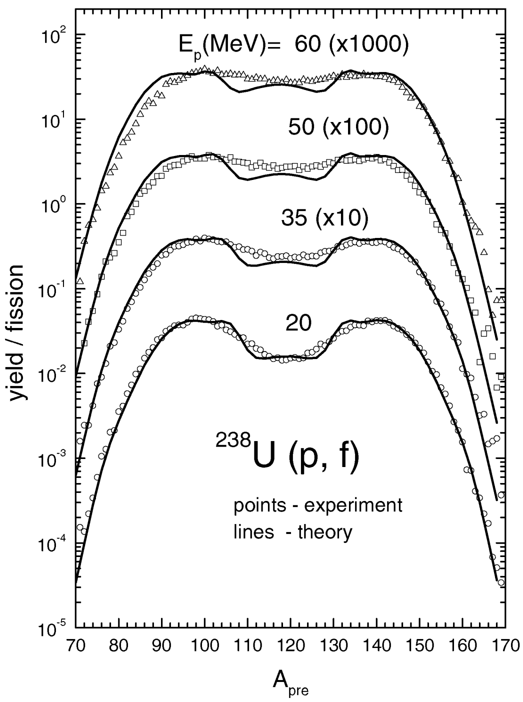

Fig. 2. Measured pre-neutron-emission fission fragment mass distributions in ^{238}U (p, f) at $E_p = 20, 35, 50$ and 60 MeV (*symbols*) and calculated ones (*curves*).

Each neutron event consisted of six parameters, three from each of the two photomultipliers at the opposite ends of PSND: time, total and fast component of the pulse charge. Standard pulse shape analysis was used to separate neutrons from γ-quanta. In the analysis of neutron events, each PSND was treated as five separate detectors. Prior to the experiment, the influence of the 2 mm stainless steel walls of the reaction chamber on the neutron spectra was measured, and energy- and position-dependent corrections were extracted. A ^{252}Cf test was always used as a reference. From the measured neutron spectra and from the well-known parameters of ^{252}Cf neutron emission, the experimental PSND efficiency was extracted. At low neutron energies (around 1 MeV) the main source of the 13% error in the energy determination is due to the uncertainty of the flight path. At higher energies (about 10 MeV) the errors are mostly due to finite time resolution (1.4 ns for all detectors) and amount to about 15%.

To extract pre- and post-scission neutron multiplicities and temperature parameters, a multiple-source procedure was used. Neutrons were assumed to be emitted isotropically in the corresponding rest-frames of three moving sources: compound nucleus and two fully accelerated fission fragments. The following fitting formula was used:

$$\frac{d^2 M_n}{dE_n\, d\Omega_n} = \frac{M_n^{pre}\sqrt{E_n \varepsilon_n}}{4\pi (T^{pre})^2}\exp\left(-\frac{\varepsilon_n}{T^{pre}}\right) + \sum_{i=1}^{2}\frac{M_{n,i}^{post}\sqrt{E_n}}{2(\pi T^{post})^{3/2}}\exp\left(-\frac{\varepsilon_n}{T^{post}}\right) \quad (1)$$

where $\varepsilon_n = E_n - 2\sqrt{E_n E_{C(F)}/A_{C(F)}}\cos(\Phi_{C(F)}) + E_{C(F)}/A_{C(F)}$; E_n is the neutron energy in laboratory system; T^{pre} the average temperature of the compound nucleus; T^{post} the average temperature of fission fragments; E_C the average kinetic energy of the compound nucleus; E_F the average kinetic energy of fission fragments; A_C the mass of the compound nucleus; A_F the average mass of a fission fragment; and $\Phi_{C(F)}$ the angle between neutron direction and compound nucleus (fragment) direction.

A nearly perfect 360° coverage in the horizontal plane allowed us to obtain a full neutron angular distribution, thus assuring good data for the fitting procedure. In the fit only neutrons with energies greater than 2 MeV were taken into account in order to reduce the influence of data points close to the registration threshold. The experimentally obtained values of pre- and post-scission and total neutron multiplicities are summarized in Table 3. The extracted fragment mass dependences of the post-scission neutron at $E_p = 20, 35, 50$, and

Table 3
Pre- and post-scission and total neutron multiplicities M_n obtained from the multiple-source fit. Errors were deduced from χ^2 behavior (increase by 3% from the minimum value)

E_{lab} (MeV)	M_n^{pre}	M_n^{post}	M_n^{tot}
20	0.87 ± 0.47	4.51 ± 0.31	5.39 ± 0.30
35	1.93 ± 0.47	4.91 ± 0.31	6.84 ± 0.30
50	2.38 ± 0.47	5.50 ± 0.31	7.80 ± 0.30
60	3.07 ± 0.47	5.60 ± 0.7	8.68 ± 0.30

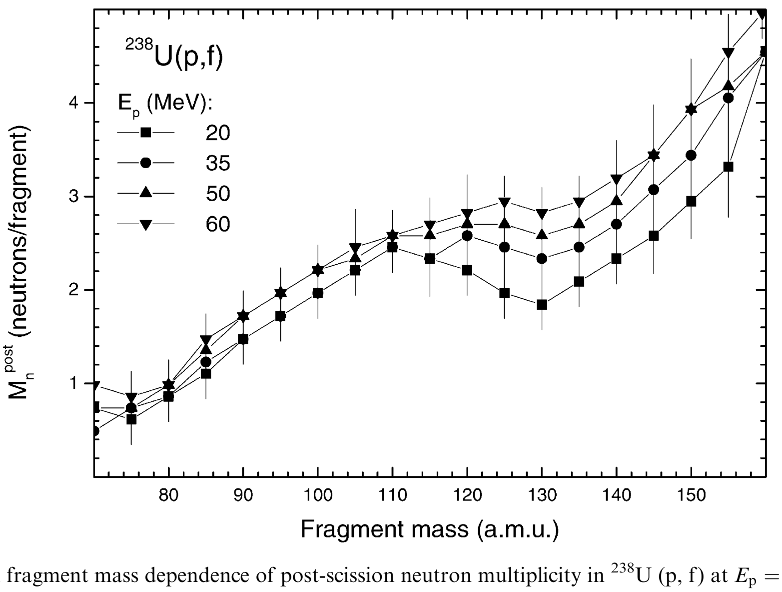

Fig. 3. Measured fission fragment mass dependence of post-scission neutron multiplicity in ^{238}U (p, f) at $E_p = 20, 35, 50$ and 60 MeV.

60 MeV are shown in Fig. 3. One can see that, with increasing exitation energy of the compound nucleus, a sawtooth structure in a dependence of $M_n^{post}(A)$ on fragment mass is washed out but that it does not reach a linear function at the higher energies we investigated. The physical reason is that excitation energy at the scission point is probably saturated at a proton energy above 50 MeV.

3. Fission product yields from measurements with IGISOL

The ion guide method developed in Jyväskylä can be successfully used for measurements of independent and cumulative fission products yields [16,20]. The new mass separator facility Ion Guide Isotope Separator On-Line (IGISOL) [21] provides us now with the possibility to investigate mass and charge distributions in the light-particle-induced fission processes. To demonstrate the abilities of the IGISOL method for measurements of the fission product yields the results recently obtained for the very asymmetric fission in proton-induced fission [3] are presented here in short form. The mass and charge distributions of the fission products from 25 MeV proton-induced fission of ^{238}U were obtained from the independent yields extracted from the measured cumulative production yields, which were determined from the radioactivity of the mass separated nuclides. Fragments following the fission of the Np compound nuclei, in the form of ions, were slowed down in high-pressure helium and transported by the flow through a differentially pumped electrode system into the acceleration stage of a mass separator. In order to maximize the production rate, the 15 mg/cm^2 thick uranium target foil was tilted to a small angle with respect to the beam axis, providing a 10-fold increase in the production rate of primary fission fragments. Radioactive ions of 40 keV energy were mass-analyzed with a resolving power of 350 and implanted into a collection tape, which was directly viewed by a set of β- and γ-ray detectors. The delay time of the ion-guide based mass separation is only of the order of ms. This allows the detection of the

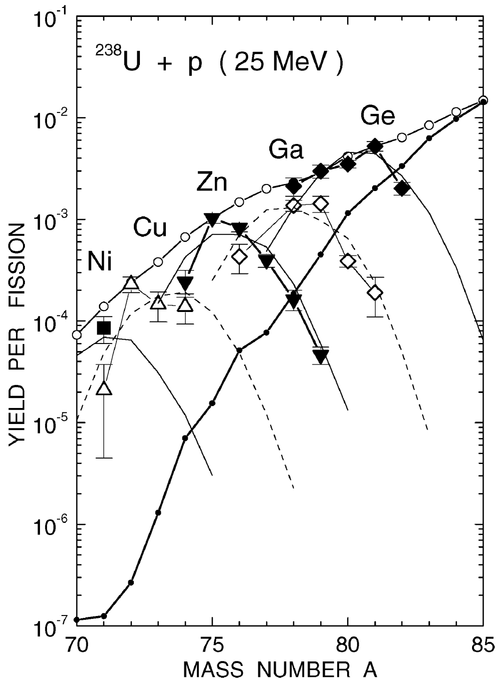

Fig. 4. Measured independent yields (*symbols with error bars*) and calculated mass yields (*open circles*) of fission products in the superasymmetric mass region in 25 MeV proton-induced fission of ^{238}U, and the mass yields (*small solid circles*) in the thermal neutron-induced fission of ^{235}U from Ref. [26]. The theoretically calculated isotopic yields are shown as thin solid and dashed lines.

shortest-lived β-radioactivities of all elements without any decay losses. Due to the fact that primary thermalized ions are initially contained in and transported by the inert helium gas, no chemical selectivity influences the transport. The total efficiency of the ion guide depends on the kinematics of the reaction involved. For example, the light fission fragment is stopped less efficiently than the heavy one. However, in this work the yield measurements were performed for the fragments in the narrow mass range with masses between 70 and 80 [3]. Thus, within the overall experimental accuracy, no corrections for kinematic effects were performed. The whole measurement series of the yields was performed with a constant proton-beam current of 3 μA. The efficiency of the whole system was regularly monitored by the yield of ^{112}Rh, which was typically 5000 ions/s. In the case of ^{71}Cu and ^{71}Ni the branchings have not yet been determined and the yields extracted represent the lower limit only. More information on the details of the data analysis can be found in Refs. [3,16]. The experimental independent yields, shown as points with error bars, for Ni, Cu, Zn, Ga and Ge isotopes, are presented in Fig. 4.

It is interesting to note that the drop in the yield from $A = 80$ down to about $A = 70$ is less than two orders of magnitude. This is drastically different from the drop observed for the thermal neutron-induced fission [26], which is also shown in Fig. 4, where the corresponding decrease in yield is about four orders of magnitude.

4. Theoretical model analysis

The experimental results on the fragment yields were analysed in the framework of a theoretical model proposed in Refs. [15–17] and used here in a more advanced version [3]. The influence of nuclear shells and charge polarization and their dependence on the excitation energy of the compound nucleus are taken into account. In comparison with the previous version of the model we introduced odd–even effects in charge and mass distributions and slightly changed the model parameters taking into account the new experimental data on very asymmetric fission [3]. Additionally, we took into account the influence of nuclear friction on fission probability and light particle evaporation on the descent from saddle to scission point by a method described in Ref. [22]. The formation cross-section of a fission product with mass number A and charge number Z can be expressed in the form

$$\sigma_f(A, Z) = \sum_{A_c Z_c} \int Y^c_{\mathrm{ind}}(A, Z) \times \mathrm{d}E_c \frac{\mathrm{d}\sigma_f(A_t, Z_t, A_p, Z_p, E_p, A_c, Z_c, E_c)}{\mathrm{d}E_c} \quad (2)$$

where subscripts t, p and c refer to target, projectile and compound nuclei, respectively, $\mathrm{d}\sigma_f/\mathrm{d}E_c$ is the partial fission cross-section of the compound nucleus at the excitation energy E_c for different fission chances over which the summing is carried out, and $Y^c_{\mathrm{ind}}(A, Z)$ is the independent yield for the given compound nucleus. The independent yields Y_{ind} are defined as the yields of fission products after light particle emission from excited primary fragments. Here we shall consider only neutron emission because at excitation energies up to about 100 MeV, the emission of protons and other charged particles is negligible with respect to the precision of available experimental data. The partial fission cross-sections are calculated in the framework of a time-dependent statistical model with inclusion of dynamical effects [22]. The compound nucleus formation cross-section is calculated by the optical model taking into account a contribution of the pre-equilibrium emission of protons and neutrons.

At low excitation energies, the primary fission fragment mass and charge distributions exhibit odd–even staggering. The primary distributions are presented in the factorisation form

$$P_{\mathrm{pre}}(Z) = \tilde{P}_{\mathrm{pre}}(Z) F_{\mathrm{oe}}(Z),$$
$$Y_{\mathrm{pre}}(A) = \tilde{Y}_{\mathrm{pre}}(A) F_{\mathrm{oe}}(A) \quad (3)$$

where $\tilde{P}_{\mathrm{pre}}(Z)$ and $\tilde{Y}_{\mathrm{pre}}(A)$ are smoothed distributions, and functions $F_{\mathrm{oe}}(Z)$ and $F_{\mathrm{oe}}(A)$ describe odd–even staggering. The calculation method of smoothed pre-neutron emission charge and mass distribution of fission fragments is described in Ref. [16]. A smoothed mass distribution is approximated by superposition of seven Gaussian distributions corresponding to different nuclear shells in fragments:

$$\tilde{Y}_{\mathrm{pre}}(A) = C_s y_s(A) + C_{a1} y_{a1}(A) + C_{a2} y_{a2}(A) + C_{a3} y_{a3}(A). \quad (4)$$

Here y_s and y_{a1}, y_{a2}, y_{a3} are symmetric and asymmetric components which present contributions from different fission modes. Each asymmetric component consists of two Gaussians representing the heavy and light fragment mass groups. The component y_{a1} is connected with the magic numbers $Z = 50$ and $N = 82$ in the heavy fragments and the superasymmetric component

y_{a3} is influenced by the nuclear shells $Z = 28$ and $N = 50$ in the light fragments. The asymmetric mode y_{a2} is supposed to be connected with the "deformed" nuclear shell at $N = 86-90$. The competition between fission modes is determined by fission dynamics and the nuclear shells in the fission fragments. The smoothed pre-neutron emission isobaric chain charge distribution is approximated by a Gaussian distribution, therefore the odd–even structure can be described by a parameter defined as a third difference of the natural logarithms of the fractional yields [27]. We consider the proton and neutron odd–even effect separately and write

$$F_{oe}(Z) \sim \exp((C_p^1 + C_p^2)\delta_z(A_c, Z_c, E_c)) \quad (5)$$

where C_p^1 and C_p^2 are defined by the parity of the proton number in the two primary fragments ($C_p = 1$ if Z is even and $C_p = -1$ if Z is odd). The proton odd–even difference parameter $\delta_z(A_c, Z_c, E_c)$ is parameterized as a function of excitation energy, charge and mass number of the compound nuclei in accordance with experimental data. Odd–even staggering in the primary mass distribution is described by the combination of proton and neutron odd–even effects. The proton and neutron odd–even difference parameters are taken to be proportional, i.e. $\delta_N(A_c, Z_c, E_c) = c\delta_z(A_c, Z_c, E_c)$ ($c < 1$). The model parameters were chosen from fitting the calculated fission fragment mass and charge distributions to experimental ones for the spontaneous and neutron- and proton-induced fission of heavy nuclei.

The calculated yields for isotopes of Ni, Cu, Zn, Ga and Ge (*solid and dashed curves*) as well as the derived mass yields (*open circles*) for the 25 MeV proton-induced fission of ^{238}U are shown in Fig. 4. Theoretical mass yields were obtained as the ratio of the calculated cross-section and the total fission cross-section with 25 MeV proton energy ($\sigma_f = 1340$ mb). For comparison, the mass yields in the thermal neutron-induced fission of ^{235}U from Ref. [26] are shown as small solid circles. One can see that the yields in the superasymmetric mass region for fission of Np compound nuclei at intermediate excitation energy differ drastically from the ones in low energy fission of ^{236}U compound nuclei. In a very asymmetric mass division at intermediate excitation energy ($E_c \geqslant 20$ MeV) there are contributions from three components: the tails from the symmetric and the second asymmetric modes and the superasymmetric mode. Enhancement of fission fragment yields in the far asymmetric region is also supported by our time-of-flight measurements, as one can see in Fig. 2 where the pre-neutron emission mass distributions in the proton-induced fission of ^{238}U at $E_p = 20, 35, 50$ and 60 MeV are displayed (*circles*) together with theoretical model predictions (*curves*). From the comparison between the experimental yields and theoretical calculations we conclude that the contribution of the superasymmetric fission mode near the nuclear shells $Z = 28$ and $N = 50$ is significant at intermediate excitation energies. Enhancement of the yields in the very asymmetric mass region proves that fission of heavy nuclei at intermediate excitation energy is a potential tool for the production of neutron-rich nuclei with $A < 80$.

The developed code allows us to calculate the energy spectra, the multiplicity distributions of the light particles emitted before scission and from fragments, and the evaporation residue cross sections. A comparison between experimental (*full symbols with error bars*) and calculated (*open symbols*) values of pre-scission, post-scission, pre-equilibrium (*line*) and total neutron multiplicities in ^{238}U (p, f) at $E_p = 20, 35, 50$ and 60 MeV is shown in Fig. 5. In these calculations we have used the energy-dependent friction coefficient in the form proposed in Ref. [28],

$$\beta(E_c) = \beta_0(c_1 T + c_2 T^2), \quad E_c > E_{th} \quad (6)$$

where $\beta_0 = 5 \times 10^{21}$ s^{-1}, and T, E_c is temperature and compound nucleus excitation energy, respectively. $E_{th} = 20$ MeV is the threshold energy, and $c_1 = 0.5$ and $c_2 = 3.0$. One can see good agreement between experimental and theoretical values of pre-scission neutron multiplicity. But there is divergence for post-scission neutron multiplicity. The calculated total neutron multiplicity includes also a pre-equilibrium part. In the fitting procedure the pre-equilibrium component is not included (see formula (1)) and one can assume that it entered in the post-scission component.

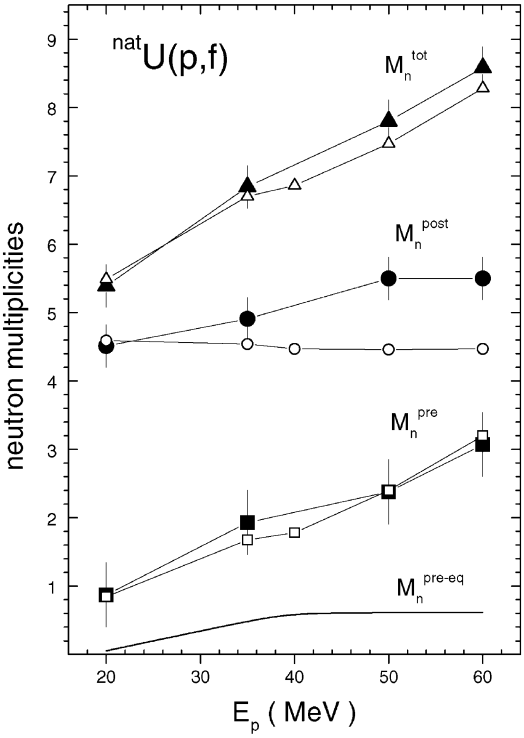

Fig. 5. Comparison between experimental (*full symbols with error bars*) and calculated (*open symbols*) values of pre-scission, post-scission, pre-equilibrium (*line*), and total neutron multiplicities in ^{238}U (p, f) at $E_p = 20, 35, 50$ and 60 MeV.

5. Conclusion

An enhancement of highly asymmetric mass and charge division in comparison with thermal neutron-induced fission is observed. A comparison of the theoretical and the experimental yields supports the hypothesis of a superasymmetric fission mode at intermediate excitation connected with $Z = 28$ and $N = 50$ shells. To make this assertion more reliable, additional investigations are needed.

One can conclude from the results obtained that proton- and neutron-induced fission of heavy nuclei at intermediate energy is a promising tool for the production of exotic neutron-rich nuclides with $A < 80$.

A model for calculating the fission product yield and the characteristics of emitted neutrons in light-particle-induced fission of heavy nuclei with inclusion of dynamical effects has been developed. This model can be used for the prediction of the formation cross-sections of exotic nuclides and for evaluation of product yields and neutron yields in fission at intermediate energy.

Experimental HENDES and IGISOL facilities can be used for measurements of the characteristics of the fission process with proton energies higher than those presented in the present paper and with other light particles. Recently, the neutron-rich fission product yields in the intermediate energy neutron-induced fission of uranium were measured using the IGISOL technique [29].

Acknowledgements

This work was supported by the Academy of Finland and the Center for International Mobility. V.A.R., D.N.V, A.V.E., and Z.R. wish to thank the Department of Physics of the University of Jyväskylä for hospitality and financial support.

References

[1] C.M. Zöller, A. Gavron, J.P. Lestone, M. Mutterer, J.P. Theobald, A.S. Iljinov, M.V. Mebel, in: C. Wagemans (Ed.), Proceedings of the Seminar on Fission "Pont d'Oye III", Castle of Pont d'Oye, Habay-la-Neuve, Belgium, 9–11 May 1995, Report EUR 16295 EN, 1995, p. 56.

[2] C.M. Zöller, Untersuchung der neutroneninduzierten Spaltung von ^{238}U im Energiebereich von 1 MeV bis 500 MeV, Ph.D. Dissertation, Technische Hochschule Darmstadt, 1995, D17, unpublished.

[3] M. Huhta, P. Dendooven, A. Jokinen, G. Lhersonneau, M. Oinonen, H. Pentillä, K. Peräjärvi, V.A. Rubchenya, J. Äystö, Phys. Lett. B 405 (1997) 230.

[4] H. Kudo et al., Phys. Rev. C 57 (1998) 178.

[5] A.C. Mueller, in: T. von Egidy, F.J. Hartmann, D. Habs, K.E.G. Löbner, H. Nifenecker (Eds.), Research with Fission Fragments", Proceedings of International Workshop, Benediktbeuern, Germany, 28–30 October 1996, World Scientific, Singapore, 1997, pp. 48–53.

[6] P. Armbruster et al., Z. Phys. A 355 (1996) 191.

[7] M. Bernas et al., Phys. Lett. B 415 (1997) 111.

[8] C.D. Bowman et al., Nucl. Instr. and Meth. A 320 (1992) 336.

[9] W. Gudowski, in: M.Kh. Khankhasaev, Zh.B. Kurmanov, H.S. Plendl (Eds.), Proceedings of International Workshop on Nuclear Methods for Transmutation of Nuclear Waste,

Dubna, Russia, 29–31 May 1996, World Scientific, Singapore, 1997, p. 3.
[10] G.D. Doolen et al., in: M.Kh. Khankhasaev, Zh.B. Kurmanov, H.S. Plendl (Eds.), Proceedings of International Workshop on Nuclear Methods for Transmutation of Nuclear Waste, Dubna, Russia, 29–31 May 1996, World Scientific, Singapore, 1997, p. 26.
[11] C.J. Bishop, R. Vandenbosch, R. Aley, R.W. Shaw Jr., I. Halpern, Nucl. Phys. A 150 (1970) 129.
[12] S. Baba, H. Umezawa, H. Baba, Nucl. Phys. A 175 (1971) 177.
[13] C.J. Bishop, I. Halpern, R.W. Shaw Jr., R. Vandenbosch, Nucl. Phys. A 198 (1972) 161.
[14] M. Strecker, R. Wien, P. Plischke, W. Scobel, Phys. Rev. C 41 (1990) 2172.
[15] E. Karttunen et al., Nucl. Sci. Eng. 109 (1991) 350.
[16] P.P. Jauho, A. Jokinen, M. Leino, J.M. Parmonen, H. Pentillä, J. Äystö, K. Eskola, V.A. Rubchenya, Phys. Rev. C 49 (1994) 2036.
[17] V.A. Rubchenya, in: M.Kh. Khankhasaev, Zh.B. Kurmanov, H.S. Plendl (Eds.), Proceedings of International Workshop on Nuclear Methods for Transmutation of Nuclear Waste, Dubna, Russia, 29–31 May 1996, World Scientific, Singapore, 1997, p. 110.
[18] J. Benlliure et al., Nucl. Phys. A 628 (1998) 458.
[19] W.H. Trzaska et al., in: J.L. Duggan, I.L. Morgan (Eds.), Application of Accelerators in Research and Industry, AIP Press, New York, 1997, p. 1059.
[20] M. Leino et al., Phys. Rev. C 44 (1991) 336.
[21] H. Penttilä et al., Nucl. Instr. and Meth. B 126 (1997) 213.
[22] V.A. Rubchenya et al., Phys. Rev. C 58 (1998) 1587.
[23] H.-G. Ortlepp et al., in: Yu. Oganessian et al. (Eds.), Proceeding of International School-Seminar on Heavy Ion Physics, Dubna, May 10–15, 1993, JINR, Dubna, Vol. 2, 1993, p. 466.
[24] A.V. Kuznetsov et al., Z. Phys. A 354 (1996) 287.
[25] A.V. Kuznetsov et al., Nucl. Instr. and Meth. A 346 (1994) 259.
[26] J.L. Sida et al., Nucl. Phys. A 502 (1989) 233c.
[27] B.L. Tracy et al., Phys. Rev. C 5 (1972) 222.
[28] D.J. Hoffman, B.B. Back, P. Paul, Phys. Rev. C 51 (1995) 2597.
[29] G. Lhersonneau et al., Eur. Phys. J. A 9 (2000) 385.